Binary Supraconductors

DOI: 10.1002/anie.201302397

# $CoBi_3$: A Binary Cobalt–Bismuth Compound and Superconductor**

*Ulrich Schwarz,* Sophie Tencé, Oleg Janson, Cevriye Koz, Cornelius Krellner, Ulrich Burkhardt, Helge Rosner, Frank Steglich, and Yuri Grin*

The metals in the sixth row of the periodic table exhibit pronounced differences to the lighter homologues because the energy levels of the valence electrons are fundamentally affected by relativistic effects.[1] Thus, post-transition elements, such as thallium, lead, and bismuth, feature the highest electron density of all metallic elements, and the pronounced spin–orbit splitting can cause the inert or the lone-pair effect. The unique properties of these metals also show in their chemical behavior; for example, most binary phase diagrams with 3d transition metals evidence the absence of compounds and wide miscibility gaps in the liquid state.[2] On the atomic scale, this thermodynamic property corresponds to the preferred formation of homoatomic contacts. Overcoming this obstacle for compound formation requires promoting heteroatomic connections, for example by treading a kinetically controlled reaction path. Alternatively, a thermodynamic stabilization of mixed atomic configurations may be realized by selecting appropriate state-variable combinations during synthesis.

The observation that a significant proportion of the few binary transition-metal–bismuth compounds exhibit superconductivity[3–7] motivated the current search for new intermetallic phases of Bi. In this study, we report the concerted experimental and theoretical investigations of the first binary compound in the cobalt–bismuth system.[2,8] The new phase is synthesized at pressures between 5.0(5) and 10(1) GPa and temperatures from 640(40) K to 1470(150) K before quenching to ambient conditions.

The maximal yield (95%) is obtained at 5 GPa and 720(50) K, that is, the reaction is realized at conditions close to the melting curve of bcc bismuth[9,10] and the transition from hcp to fcc cobalt.[10,11] The molar volume of the binary compound is 10% smaller at ambient conditions (2% at 5 GPa) than the sum of the elemental increments.[12] Therefore, the realization of phase formation by application of high pressure is in full accordance with Le Chatelier's principle.

[*] Priv.-Doz. Dr. U. Schwarz, Dr. S. Tencé, Dr. O. Janson, C. Koz, Prof. Dr. C. Krellner, Dr. U. Burkhardt, Dr. H. Rosner, Prof. Dr. F. Steglich, Prof. Yu. Grin
MPI für Chemische Physik fester Stoffe
Nöthnitzer Strasse 40, 01187 Dresden (Germany)
E-mail: schwarz@cpfs.mpg.de

[**] The authors thank Susan Leipe for high-pressure preparation, Dr. Stefan Hoffmann and Susann Scharsach for DSC measurements, and Sylvia Kostmann, Monika Eckert and Petra Scheppan for metallographic investigations. Dr. Christoph Geibel, Dr. Walter Schnelle, Dr. Yurii Prots, and Prof. Dr. Michael Ruck (TU Dresden) are gratefully acknowledged for helpful discussions.

Supporting information for this article is available on the WWW under http://dx.doi.org/10.1002/anie.201302397.

At ambient pressure, optical metallography reveals only a single binary reaction product of the high-pressure synthesis (Supporting Information, Figure S1), and electron-probe studies (Supporting Information, Figure S2) reveal its composition as $Co_{1.00(1)}Bi_{3.00(1)}$. The phase decomposes exothermally at about 500 K (Supporting Information, Figure S3) into elemental cobalt and bismuth, which manifests the metastable character of the binary compound.

The cobalt compounds of the lighter analogues, namely $CoP_3$, $CoAs_3$, and $CoSb_3$, all form skutterudite-type arrangements,[13] whereas $CoBi_3$ forms a $NiBi_3$-like motif.[14,15] Results of the crystal structure refinement[16] (Supporting Information, Figure S4 and Tables S1–S3) show that in the structure pattern (Figure 1, top) cobalt atoms are coordinated by seven bismuth atoms in the form of a monocapped trigonal prism. These polyhedra condense into one-dimensional building units by sharing prism faces. The resulting $[CoBi_{6/3}Bi]$ columns are arranged in the form of a distorted hexagonal rod packing. This unusual structure pattern and especially the occurrence of short distances $d$(Co-Co) within the interconnected segments (Figure 1, top) motivated an investigation of the atomic interactions with quantum-chemical methods.

Application of the quantum theory of atoms in molecules (QTAIM[18]) reveals atomic basins with complex shapes (Figure 1, bottom) comprising 27.0 electrons for Co, 82.8 for Bi1 and for Bi2, and 83.4 for Bi3. Taking into account the atomic numbers of 27 for Co and 83 for Bi, this corresponds to essentially uncharged atoms, in full agreement with the small electronegativity differences of the elements.[19]

The distribution of the electron-localizability indicator (ELI-D[20]) within the inner shell of the cobalt atoms exhibits deviations from spherical symmetry (Figure 2, top). The topological organization of the short contact $d$(Co–Bi1) is taken as a fingerprint for covalent interactions. The absence of definitive ELI-D maxima on the contacts $d$(Co–Co) imply that the short interatomic distances are caused indirectly by the Co–Bi and not by direct Co–Co interactions. Clear ELI-D attractors close to the bismuth atoms, which show lone-pair-like shapes, are located at the outer face of the columns (Figure 2, bottom). Consequently, the crystal structure is organized by covalent heteroatomic Co–Bi interactions within the columns complemented by lone-pair-like interactions between these one-dimensional building units. These findings are in agreement with the earlier observation that even chemical modification of the structure motif, for example by subtle oxidation in the sub-iodide $Bi_3NiI_{0.75}$, leaves the covalently bonded columns intact.[21]

The sectors of different interaction types are separated by periodic nodal surfaces (PNS; Figure 3, top).[22a] A PNS separates the region in which the atoms are linked by covalent

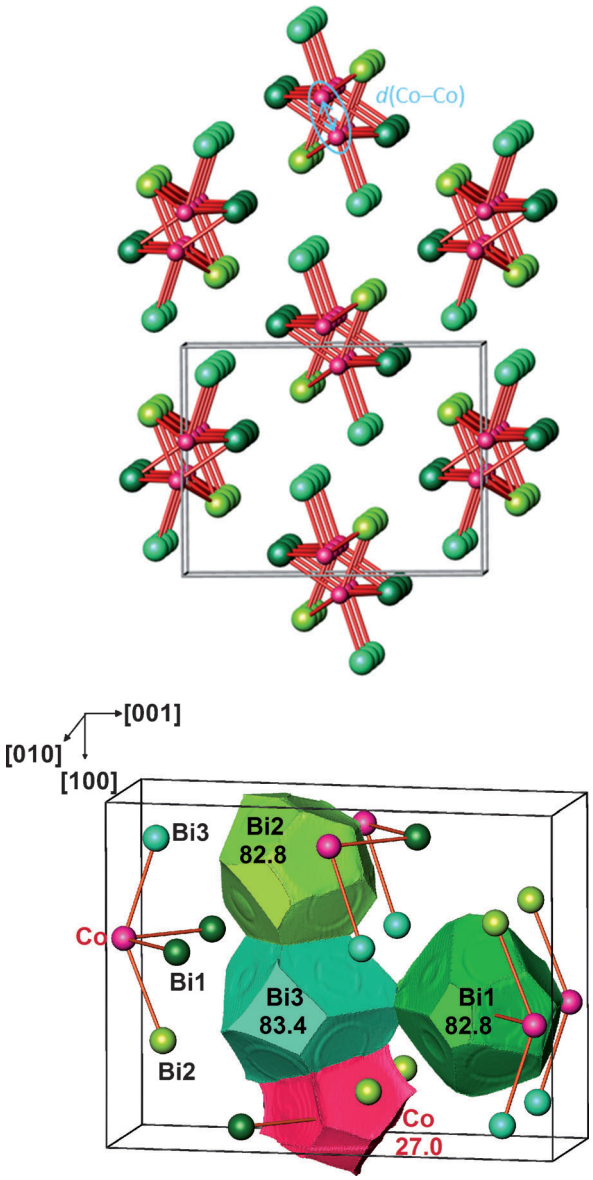


***Figure 1.*** Top: Crystal structure of $CoBi_3$ in a projection along [010]. Red spheres indicate the transition metal atoms; the different bismuth species are shown in different shades of green. The seven shortest distances *d*(Co–Bi) between 2.688(2) and 2.780(3) Å are designated by red lines. Two additional short distances *d*(Co–Co)of 2.612(3) Å (indicated by the light blue double arrow) complement the coordination of the transition metal atoms. These short distances *d*(Co–Bi) and *d*(Co–Co) do not exceed the sum of the elemental radii[17] more than 5%. Bottom: QTAIM[18] atomic basins in $CoBi_3$. The calculated electron populations basically correspond to the nuclear charges of the elements.

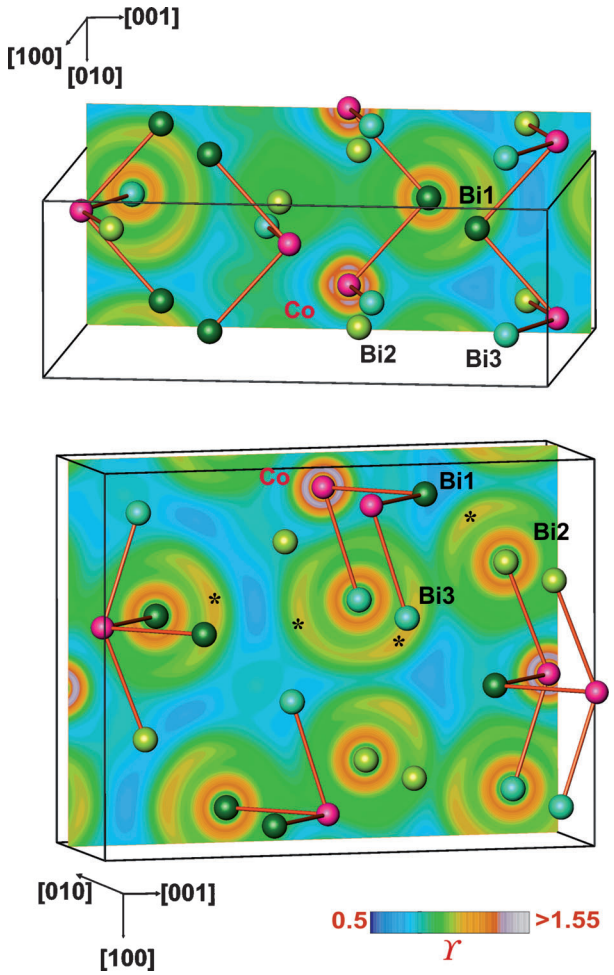


***Figure 2.*** Electron localizability indicator Y of $CoBi_3$: Top: distribution of ELI-D in the plane of the Co–Bi1 contacts; Bottom: distribution of ELI-D in the plane of the Co–Bi2 and Co–Bi3 contacts. Some lone-pair-like attractors are marked by asterisks.

bonds from the compartment between the columnar units that contains the lone-pair-shaped attractors. The covalent building units are conventional one-dimensional motifs in $CoBi_3$. The rhodium compound $RhBi_4$ exhibits the same partitioning principle, but here three-dimensional frameworks form a hyperbolic layer-type structure of interpenetrating networks (Figure 3, bottom).[22b]

Electrical resistivity measurements of polycrystalline $CoBi_3$ samples reveal metal-like temperature dependence with an onset of superconductivity at $T_c = 0.48$ K (Figure 4). This transition shows in an anomaly of the specific heat (Figure 4) with the magnitude of the effect ("jump height") evidencing bulk superconductivity ($\Delta C_p/T$ of the order 20 mJ mol$^{-1}$ K$^{-2}$).

The determined Debye temperature[23] of $CoBi_3$ (124 K) corresponds approximately to that of $NiBi_3$ (144 K[4]). This finding is consistent with highly similar phonon spectra of both compounds originating from isotypic crystal structures with related lattice parameters and insignificantly different average molecular masses. Provided that comparable DOS values exist at the Fermi level, this would correspond to akin critical temperatures, for example, according to the phenomenological description for electron-phonon coupled superconductors.[25] However, the superconducting transition temperature of $NiBi_3$ is considerably higher ($T_c = 4.0$ K) than that of $CoBi_3$. This remarkable discrepancy was inspected more closely by a theoretical treatment of the electronic structure.

To estimate the effect of spin–orbit (SO) coupling in the heavy metal compounds, both scalar and fully relativistic DFT

  

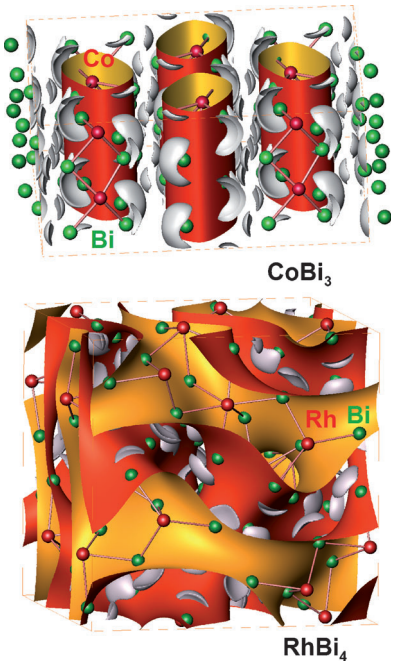


***Figure 3.*** Crystal structures, periodic nodal surfaces,[22a] and lone-pair-shaped ELI-D[20] attractors of $CoBi_3$ (top) and $RhBi_4$[22b] (bottom). The columns in $CoBi_3$ which are located right and left in front are shown without the enveloping PNS.

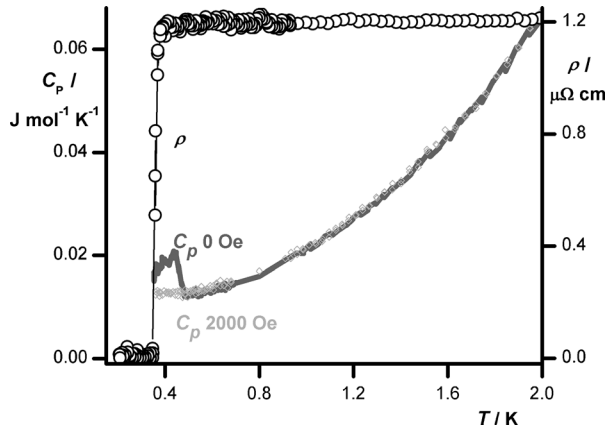


***Figure 4.*** Heat capacity $C_p$ and electrical resistivity $\rho$ of $CoBi_3$ at low temperatures $T$. Discontinuous changes at 0.48 K indicate the transition into the superconducting state.[24] $C_p$ data measured in a magnetic field of 2000 Oe, at which superconductivity is completely suppressed, are measured as a reference baseline.

band-structure computations were carried out. At the Fermi energy ($E_F$) of $CoBi_3$, both Bi6p and Co3d states contribute almost equally to the electronic density of states (DOS, Figure 5). The significant amount of Co3d states that is additionally promoted by the SO splitting (inset of Figure 5) approaches the limit for band (itinerant) magnetism. Such a magnetic instability is equivalent to strong spin fluctuations, and these impede the formation of Cooper pairs. Therefore, the substantial decrease of $T_c$ in $CoBi_3$ is finally attributed to the high density of Co3d states at $E_F$. This assignment is fully compatible with the observation that $NiBi_3$ (showing a considerably higher $T_c$) exhibits a lower total density of states and only about 1/3 Ni3d contributions at $E_F$ (Supporting Information, Figure S5). Both features concordantly reduce the density of the transition metal 3d states at the Fermi energy. In agreement with these results, a substitution of cobalt with nickel preserves a non-magnetic state, whereas the exchange of cobalt with iron gives rise to magnetic order (Supporting Information, Figure S6).

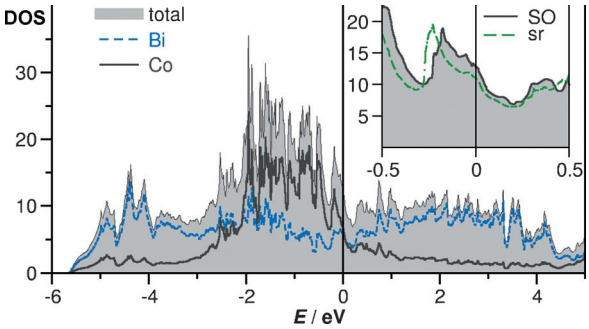


***Figure 5.*** Calculated electronic density of states (DOS) referring to the number of states per unit cell and electron volt as a function of energy $E$. The Fermi level ($E_F$) is set to zero energy. The states at $E_F$, which are crucial for superconductivity, are essentially Co3d and Bi6p states. The Bi atoms, although located on different crystallographic positions, provide analogue contributions to the DOS. The inset shows a comparison of the DOS in the vicinity of $E_F$ obtained by a scalar relativistic (marked sr) and a fully relativistic (labeled SO) treatment of the spin–orbit coupling.

Regarding the pressure-induced changes, both solid Co and Bi exhibit only minor changes of the orbital population numbers upon moderate compression (Supporting Information, Tables S4 and S5).[26] This behavior is in substantial contrast to heavy s metals, such as Cs[27] or Ba,[28] or electron-poor transition metals, such as Sc[29] or La.[30] The electronic DOS of cobalt remains essentially unaffected by the hcp to fcc transition and the compression to 5 GPa (Supporting Information, Figures S7 and S8). For the heavy metal bismuth, the fully relativistic treatment reveals pronounced spin–orbit splitting (Supporting Information, Figure S9) and reliably reproduces the pressure-induced semiconductor-to-metal transition close to 5 GPa (Supporting Information, Figure S10). In both elemental Bi and bismuth-rich $CoBi_3$, the lower band edge of the (bonding) Bi6p states is shifted by approximately −0.6 eV upon pressure increase to 5 GPa (Supporting Information, Figures S10 and S11).

In conclusion, high-pressure high-temperature synthesis is a beneficial method in overcoming the obstacles of compound formation in systems of basically immiscible metals. Considering the large number of binary phase diagrams with extended miscibility gaps, a perspective for gaining access to new metastable intermetallic compounds becomes apparent.

## Experimental Section

Sample preparation before and after compression was realized in argon-filled glove boxes ($p(H_2O) \approx 0.1$ ppm and $p(O_2) \approx 0.1$ ppm). Powders of bismuth (99.999%, 100 μm mesh) and cobalt (99.99%, 200 mesh) were mixed and ball-milled using a substance amount

  

fraction of Bi/Co = 3:1. High pressures were generated by means of an octahedral multi-anvil press[31] equipped with boron nitride crucibles. To determine the optimal conditions of formation, the mixtures of Bi and Co were exposed to pressures of 5 GPa or 10 GPa for several hours at temperatures between 370 °C and 1200 °C. After cooling to room temperature, the pressure was released. The polished microstructures of the products were analyzed by light-optical and scanning-electron microscopy using a Philips XL30 instrument ($LaB_6$ cathode, acceleration voltage 30 kV). The compositions were determined by wavelength dispersive X-ray spectroscopy with Co and Bi as references. Differential thermal analysis (DTA) was performed with a Netzsch DSC 404 C instrument using Pt-Rh crucibles in the temperature range from 298 K to 953 K with a heating rate of 10 K $min^{-1}$.

X-ray powder diffraction data were collected at room temperature in transmission alignment with a Huber Image Plate Guinier Camera G670 using Cu-$K\alpha1$ radiation ($\lambda = 1.54056$ Å, $2° \le 2\theta \le 100°$, $\Delta 2\theta = 0.005°$). Lattice and structural parameters were refined using complete diffraction profiles (Rietveld method) by means of the computer program WinCSD.[16] Measurements of the physical properties were realized with polycrystalline sample pieces. Electrical resistivity was measured between 0.33 K and 300 K by an alternating current four-point method utilizing a Quantum Design PPMS with a $^3$He insert. Specific-heat measurements were carried out between 0.35 K and 300 K by a relaxation method using a PPMS.

Density-functional theory (DFT) band-structure calculations were performed using the full-potential code FPLO9.01-35.[32] For the exchange and correlation potential, local density approximation (LDA) and generalized gradient approximation (GGA) parameterizations were used.[33,34] Spin–orbit coupling was taken into account by solving the full four-component Dirac equation. Spin-polarized calculations employed a 14080-points $k$-mesh (2277 points in the irreducible wedge). All calculations were carefully checked for convergence. Doping on the Co and Bi sites was modeled using the virtual crystal approximation.[35] The calculated electron densities were processed by the computer program DGrid.[36]

Received: March 21, 2013
Revised: May 22, 3013
Published online: July 23, 2013

**Keywords:** bismuth · cobalt · high-pressure reactions · relativistic effects · superconductivity

[1] P. Pykkö, *Chem. Rev.* **1988**, *88*, 563.
[2] T. B. Massalki, *Binary Alloy Phase Diagrams*, ASM, Metals Park, OH, **1986**.
[3] a) N. E. Alekseevskii, N. B. Brandt, T. I. Kostina, *Bull. Acad. Sci. URSS* **1952**, *16*, 233; b) N. E. Alekseevskii, N. B. Brandt, T. I. Kostina, *J. Exp. Theor. Phys.* **1951**, *21*, 951.
[4] Y. Fujimori, S. Kan, B. Shinozaki, T. Kawaguti, *J. Phys. Soc. Jpn.* **2000**, *69*, 3017.
[5] F. Weitzer, W. Schnelle, R. Cardoso Gil, S. Hoffmann, R. Giedigkeit, Yu. Grin, *CALPHAD* **2009**, *33*, 27.
[6] T. Herrmannsdörfer, R. Skrotzki, J. Wosnitza, D. Kohler, R. Boldt, M. Ruck, *Phys. Rev. B* **2011**, *83*, 140501.
[7] J. Kumar, A. Kumar, A. Vajpayee, B. Gahtori, D. Sharma, P. K. Ahluwalia, S. Auluck, V. P. S. Awana, *Supercond. Sci. Technol.* **2011**, *24*, 085002.
[8] a) A. Lewkonja, *Anorg. Chem.* **1908**, *59*, 315; b) F. Ducelliez, *Bull. Soc. Chim. Fr.* **1909**, *5*, 61; c) W. Koster, E. Zorn, *Z. Metallkd.* **1952**, *43*, 333; d) M. Hansen, K. Anderko, *Constitution of Binary Alloys*, 2nd ed., McGraw-Hill Book Comp., New York, **1958**; e) R. Damm, E. Scheil, E. Wachtel, *Z. Metallkd.* **1962**, *53*, 196.
[9] W. Klement, G. C. Kennedy, A. Jayaraman, *Phys. Rev.* **1963**, *131*, 632.
[10] G. C. Kennedy, R. C. Newton in *Solids Under Pressure* (Eds.: W. Paul, D. W. Warschauer), McGraw-Hill, New York, **1963**, chap. 7.
[11] a) A. Fernández Guillermet, *Int. J. Thermophys.* **1987**, *8*, 481; b) T. Nishizawa, K. Ishida, *Bull. Alloy Phase Diag.* **1983**, *4*, 387.
[12] For the most recent crystal structure refinements of cobalt, see: a) V. G. Kuznetsov, M. A. Sokolova, K. K. Palkina, Z. V. Popova, *Inorg. Mater.* **1965**, *1*, 617; b) M. C. Cadeville, *Solid State Commun.* **1970**, *8*, 847; c) W. Zarek, A. Winiarska, A. Ogrodnik, A. Chelkowski, *Acta Phys. Pol. A* **1978**, *53*, 397; d) H. Masumoto, K. Watanabe, K. Inagawa, *Trans. Jpn. Inst. Met.* **1976**, *17*, 592; e) F. Aldinger, S. Jönsson, *Z. Metallkde.* **1977**, *68*, 362; f) K. H. J. Buschow, P. G. van Engen, R. Jongebreur, *J. Magn. Magn. Mater.* **1983**, *38*, 1; for bismuth, see: g) A. A. Sher, I. P. Odin, A. V. Novoselova, *Russ. J. Inorg. Chem.* **1986**, *31*, 435; h) B. C. Giessen, M. Morris, N. J. Grant, *Trans. Metall. Soc. AIME* **1967**, *239*, 883; for a summary of older results on both elements, see: i) J. Donohue, *The structures of the elements*, Krieger Publishing, Malabar, **1982**.
[13] a) N. Mandel, J. Donohue, *Acta Crystallogr. Sect. B* **1971**, *27*, 2288; b) A. Kjekshus, T. Rakke, *Acta Chem. Scand. Part A* **1974**, *28*, 99; c) J. Ackermann, A. Wold, *J. Phys. Chem. Solids* **1977**, *38*, 1013; d) T. Rosenqvist, *Acta Metall.* **1953**, *1*, 761; e) N. N. Zhuravlev, G. S. Zhdanov, R. N. Kuz'min, *Sov. Phys. Crystallogr.* **1960**, *5*, 532; f) T. Schmidt, G. Kliche, H. D. Lutz, *Acta Crystallogr. Sect. C* **1987**, *43*, 1678.
[14] $CoBi_3$: Space group *Pnma*, $a = 8.8464(7)$, $b = 4.0697(4)$, $c = 11.5604(9)$ Å from powder diffraction data, $Z = 4$, $R_B = 0.046$ with $2\theta_{max} = 101.3°$). Co (0.090(1), 1/4, 0.520(1)), Bi1 (0.4101(5), 1/4, 0.1782(1)); Bi2 (0.2974(1), 1/4, 0.8929(3)); Bi3 (0.3833(5), 1/4, 0.5928(4)). For details, see the Supporting Information, Tables S1a–c and Figure S4.
[15] a) H. Fjellvåg, S. Furuseth, *J. Less-Common Met.* **1987**, *128*, 177; b) M. Ruck, T. Söhnel, *Z. Naturforsch. B* **2006**, *61*, 785.
[16] L. G. Akselrud, P. Y. Zavalii, Y. N. Grin, V. K. Pecharsky, B. Baumgartner, E. Woelfel, *Mater. Sci. Forum* **1993**, *133–135*, 335.
[17] J. Emsley, *The Elements*, Clarendon, Oxford, **1991**.
[18] R. F. W. Bader, *Atoms in molecules*, Oxford University Press, Oxford, **1990**.
[19] The most frequently used electronegativity values for Co and Bi, respectively, correspond to 1.8 and 2.02 (Pauling), 1.70 and 1.67 (Allred–Rochow), or 4.3 eV and 4.69 eV (absolute).[17]
[20] ELI-D illustrates the average number of electrons (charge) per fixed fraction of a same-spin electron pair in each point of real space; see: a) M. Kohout, *J. Quantum Chem.* **2004**, *97*, 651; b) M. V. Butovskii, C. Döring, V. Bezugly, F. R. Wagner, Yu. Grin, R. Kempe, *Nat. Chem.* **2010**, *2*, 741; c) M. Kohout, F. R. Wagner, Yu. Grin, *Int. J. Quantum Chem.* **2006**, *106*, 1499; d) F. R. Wagner, V. Bezugly, M. Kohout, Yu. Grin, *Chem. Eur. J.* **2007**, *13*, 5724; e) F. R. Wagner, M. Kohout, Yu. Grin, *J. Phys. Chem. A* **2008**, *112*, 9814.
[21] M. Ruck, *Z. Anorg. Allg. Chem.* **1997**, *623*, 243.
[22] a) H. G. von Schnering, R. Nesper, *Z. Phys. B* **1991**, *83*, 407; b) Yu. Grin, U. Wedig, H. G. von Schnering, *Angew. Chem.* **1995**, *107*, 1318; *Angew. Chem. Int. Ed. Engl.* **1995**, *34*, 1204.
[23] With the experimental parameter for $\alpha$ determined by a fit of a Sommerfeld–Debye polynomial $C_p = \gamma T + \alpha T^3$, the Debye temperature $\theta_D$ is calculated according to $\theta_D = (12\pi^4 \times n \times N_A \times k_b/5\alpha)^{1/3}$. Here, $n$ is the number of atoms per formula unit, $N_A$ the Avogadro number, and $k_B$ the Boltzmann constant.
[24] The $C_p(T)$ curve in the normal state reaches a constant value when tending towards zero temperature. It remains to be investigated whether the observed behavior is an experimental artifact or an intrinsic property of the investigated samples because of magnetic hyperfine contributions of cobalt; see, for

  

example: N. E. Phillips, *CRC Crit. Rev. Solid State Sci.* **1971**, *2*, 467.

[25] The electron-phonon coupling $\lambda_{e\text{-}ph}$ which determines the attractive part of the Cooper pair bonding, can be estimated by the formula $\lambda_{e\text{-}ph} = [1.04 + \mu^* \ln(\theta_D/1.45\,T_c)]/[(1-0.62\mu^*)\ln(\theta_D/1.45\,T_c) - 1.04]$, in which $T$c is the critical temperature, $\theta_D$ the Debye temperature, and $\mu^*$ the Coulomb pseudopotential, which is usually fixed empirically to 0.13; see: W. L. McMillan, *Phys. Rev.* **1968**, *167*, 331.

[26] a) R. E. Cohen, S. Gramsch, G. Steinle-Neumann, L. Stixrude in *High Pressure Phenomena* (Ed.: R. J. Hemley et al.), Proceedings of the International School of Physics Enrico Fermi, Course CXLVII (Society Italiana di Fisica), Bologna, **2002**, p. 215; b) U. Häussermann, K. Söderberg, R. Norrestam, *J. Am. Chem. Soc.* **2002**, *124*, 15359; c) Y. Shoaib Mohammed, Y. Yan, H. Wang, K. Li, X. Du, *J. Magn. Magn. Mater.* **2010**, *322*, 653.

[27] a) R. Sternheimer, *Phys. Rev.* **1950**, *78*, 235; b) A. K. McMahan, *Phys. Rev. B* **1978**, *17*, 1521; c) D. Glötzel, A. K. McMahan, *Phys. Rev. B* **1979**, *20*, 3210; d) A. K. McMahan, *Phys. Rev. B* **1984**, *29*, 5982; e) U. Schwarz, K. Takemura, M. Hanfland, K. Syassen, *Phys. Rev. Lett.* **1998**, *81*, 2711; f) U. Schwarz, O. Jepsen, K. Syassen, *Solid State Commun.* **2000**, *113*, 643; g) S. G. Louie, M. L. Cohen, *Phys. Rev. B* **1974**, *10*, 3237.

[28] a) J. A. Moriarty, *Phys. Rev. B* **1986**, *34*, 6738; b) W-S. Zeng, V. Heine, O. Jepsen, *J. Phys. Condens. Matter* **1997**, *9*, 3489; c) S. K. Reed, G. J. Ackland, *Phys. Rev. Lett.* **2000**, *84*, 5580; d) I. Loa, R. J. Nelmes, L. F. Lundegaard, M. I. McMahon, *Nat. Mater.* **2012**, *11*, 627.

[29] a) A. Ormeci, K. Koepernick, H. Rosner, *Phys. Rev. B* **2006**, *74*, 104119; b) J. J. Hamlin, J. S. Schilling, *Phys. Rev. B* **2007**, *76*, 012505.

[30] A. K. McMahan, H. L. Skriver, B. Johansson, *Phys. Rev. B* **1981**, *23*, 5016.

[31] D. Walker, M. A. Carpenter, C. M. Hitch, *Am. Mineral.* **1990**, *75*, 1020.

[32] K. Koepernik, H. Eschrig, *Phys. Rev. B* **1999**, *59*, 1747.

[33] J. P. Perdew, Y. Wang, *Phys. Rev. B* **1992**, *45*, 13244.

[34] J. P. Perdew, K. Burke, M. Ernzerhof, *Phys. Rev. Lett.* **1996**, *77*, 3865.

[35] D. Kasinathan, M. Wagner, K. Koepernik, R. Cardoso-Gil, Yu. Grin, H. Rosner, *Phys. Rev. B* **2012**, *85*, 035207.

[36] M. Kohout, computer program DGrid, version 4.6, Radebeul, Germany, **2011**.

  